


RESEARCH PAPER

Quantitative systems pharmacology analysis of drug combination and scaling to humans: the interaction between noradrenaline and vasopressin in vasoconstriction

Correspondence Piet H van der Graaf, Certara QSP, Canterbury Innovation Centre, Unit 43, University Road, Canterbury CT2 7FG, UK. E-mail: piet@certara.com

Received 18 May 2018; Accepted 27 May 2018

Anyue Yin^{1,2} , Akihiro Yamada^{1,3}, Wiros B Stam⁴, Johan G C van Hasselt¹ and Piet H van der Graaf^{1,5}

¹Division of Systems Biomedicine and Pharmacology, Leiden Academic Centre for Drug Research (LACDR), Leiden University, Leiden, The Netherlands, ²Department of Clinical Pharmacy and Toxicology, Leiden University Medical Centre, Leiden, The Netherlands, ³Clinical Pharmacology PKMS Group, Astellas Pharma Inc., Tokyo, Japan, ⁴Dutch Ministry of Health and Sports, Den Haag, The Netherlands, and ⁵Certara QSP, Canterbury, UK

BACKGROUND AND PURPOSE

Development of combination therapies has received significant interest in recent years. Previously, a two-receptor one-transducer (2R-1T) model was proposed to characterize drug interactions with two receptors that lead to the same phenotypic response through a common transducer pathway. We applied, for the first time, the 2R-1T model to characterize the interaction of noradrenaline and arginine-vasopressin on vasoconstriction and performed inter-species scaling to humans using this mechanism-based model.

EXPERIMENTAL APPROACH

Contractile data were obtained from *in vitro* rat small mesenteric arteries after exposure to single or combined challenges of noradrenaline and arginine-vasopressin with or without pretreatment with the irreversible α -adrenoceptor antagonist, phenoxybenzamine. Data were analysed using the 2R-1T model to characterize the observed exposure–response relationships and drug–drug interaction. The model was then scaled to humans by accounting for differences in receptor density.

KEY RESULTS

With receptor affinities set to published values, the 2R-1T model satisfactorily characterized the interaction between noradrenaline and arginine-vasopressin in rat small mesenteric arteries (relative standard error $\leq 20\%$), as well as the effect of phenoxybenzamine. Furthermore, after scaling the model to human vascular tissue, the model also adequately predicted the interaction between both agents on human renal arteries.

CONCLUSIONS AND IMPLICATIONS

The 2R-1T model can be of relevance to quantitatively characterize the interaction between two drugs that interact *via* different receptors and a common transducer pathway. Its mechanistic properties are valuable for scaling the model across species. This approach is therefore of significant value to rationally optimize novel combination treatments.

Abbreviations

2R-1T, two-receptor one-transducer; AIC, Akaike information criterion; AVP, arginine-vasopressin; C_H , receptor density in human vessels; C_R , receptor density in rat vessels; E/[A], concentration-effect; E_{max} , maximum effect; FIH, first-in-human; GOF, goodness-of-fit; IIV, inter-individual variability; K , the total transducer amount at half-maximal effect; K_{AVP} , affinity of AVP on V_{1A} receptors; KHS, Krebs–Henseleit solution; K_{NA} , affinity of noradrenaline on α_{1A} -adrenoceptors; m_{AVP}/K , maximum transducer amount that AVP can produce normalized by K ; m_{NA}/K , maximum transducer amount that noradrenaline can produce normalized by K ; n_{AVP} , Hill slope index of AVP transduction pathway; n_H , Hill slope index of E/[A] curve; n_M , Hill slope index of the common transduction pathway; n_{NA} , Hill slope index of noradrenaline transduction pathway; PBZ_A , phenoxybenzamine effect on α_{1A} -adrenoceptors; PBZ_M , phenoxybenzamine effect on the common transducer; pEC_{50} , midpoint location of E/[A] curve; RSE, relative standard error; SMA, small mesenteric artery; VPC, visual predictive check

Introduction

The increasing availability of targeted therapeutic agents has raised interest in rationally developing combination therapies associated with improved efficacy profiles or reduction of side effects (Fitzgerald *et al.*, 2006; Al-Lazikani *et al.*, 2012). However, the identification and characterization of optimal drug combination regimens are not straightforward. Mathematical approaches to characterize pharmacological interactions between drugs have shown to be of significant relevance to address this challenge (Jonker *et al.*, 2005; Danhof *et al.*, 2007; Van Hasselt and Van Der Graaf, 2015; Gabrielsson *et al.*, 2016; Koch *et al.*, 2016).

The interaction of two agonists that lead to a single phenotypic response through different receptors and a common transduction pathway is one common type of drug–drug interaction. For such an interaction, a theoretical mechanism-based model was proposed three decades ago (Leff, 1987). According to the geometry of the agonist concentration-effect ($E/[A]$) curve, this two-receptor one-transducer (2R-1T) model can account for phenomena like threshold amplification and potentiation and predicts the conditions under which they will occur (Christ and Jean-Jacques, 1991; Gerthoffer, 1996). Previously, a model based on these principles was used to describe the effect of a single agonist acting simultaneously at two different receptors linked to a common transduction pathway (Van der Graaf *et al.*, 1996). Scaramellini then extended this model to allow for the interacting agonists to have $E/[A]$ curves with different slopes (Scaramellini *et al.*, 1997). This approach provides a framework that can describe another mechanism of drug–drug interaction besides other commonly used mechanism-based methodologies that focus primarily on the effect of two drugs acting on one receptor (Koch *et al.*, 2016). However, there is still a lack of research on the application of this framework.

Experimental models for drug-induced vasoconstriction have been extensively used to quantitatively investigate agonist–agonist interactions (Prins *et al.*, 1992; Cohen and Schenck, 2000; Lemos *et al.*, 2002; Segarra *et al.*, 2002; Streefkerk *et al.*, 2003). In the present study, we focused on the pharmacological interaction between **arginine-vasopressin (AVP)** and **noradrenaline**. Noradrenaline and AVP are two endogenous molecules involved in cardiovascular regulation as well as being used as clinical therapeutic agents to constrict blood vessels. Noradrenaline is a typical treatment for septic shock where AVP can be added with the intent of raising blood pressure or decreasing noradrenaline dosage (Dellinger *et al.*, 2013). We assessed if the previously described theoretical 2R-1T framework can be used to characterize the interaction between noradrenaline and AVP on blood vessel contraction. Rat small mesenteric artery (SMA) was chosen as the model system, for which it is known that vasoconstriction induced by AVP and noradrenaline is associated with the **V_{1A} vasopressin receptor** (Stam *et al.*, 1998) and the **α_{1A}-adrenoceptor** (Stam *et al.*, 1999; Pérez-Rivera *et al.*, 2007), respectively, involving a common transduction pathway (Mauger *et al.*, 1984). Furthermore, we also investigated if the mechanism-based basis of the 2R-1T model can be utilized to allow for translational inter-species scaling to humans.

As far as we know, the present paper is the first account of an application of the 2R-1T model and its use in translational pharmacology.

Methods

Animals

All animal care and experimental protocols were approved by the local Animal Experiments Committee, under the Dutch National Experiments on Animals Act. Animal studies are reported in compliance with the ARRIVE guidelines (Kilkenny *et al.*, 2010; McGrath and Lilley, 2015), and United States NIH guidelines. Male Wistar rats, a commonly used rat strain in pharmacological studies, were obtained from Harlan, Zeist, The Netherlands.

Rat small mesenteric artery (SMA) preparation. Male Wistar rats (250–350 g, 6–12 weeks) were anaesthetized (sodium pentobarbitone, 60 mg·kg⁻¹, i.p.) and killed by cervical dislocation. The mesentery was removed and placed in ice-cold modified Krebs–Henseleit solution (KHS) of the following composition (mM): NaCl 119.0, NaHCO₃ 25.0, KCl 4.7, KH₂PO₄ 1.2, MgSO₄ 1.2, glucose 5.5, CaCl₂ 2.5, and EDTA 0.026. Arterial trees were dissected and cleared from surrounding adipose tissue. From each arterial tree, a ring segment (~2 mm in length) was mounted in a myograph (J. P. Trading, Aarhus, Denmark) with separated 6 mL organ baths containing modified KHS at 37°C. The KHS was continuously gassed with 95% O₂ and 5% CO₂, as described previously (Mulvany *et al.*, 1977). Tissue responses were measured continuously as changes in isometric force.

Following a 30 min stabilization period, the internal diameter of each vessel was set to a tension equivalent to 0.9 times the estimated diameter at 100 mmHg effective transmural pressure ($I_{100} = 200\text{--}300\ \mu\text{m}$) according to the standard procedure of Mulvany & Halpern (Mulvany *et al.*, 1977). After a further 30 min stabilization period, the preparations were challenged five times with noradrenaline (10 μM) with washouts after each challenge. The presence of the endothelium was confirmed by adding with 10 μM of methacholine after the first challenge and tissues which responded with less than 60% relaxation were rejected. The contraction induced by the fifth noradrenaline challenge was regarded as a calibration contraction in the experiment, relative to which all subsequent responses were expressed. This normalization eliminated absolute contractile power differences between vessel segments that result from for example smooth muscle content of the segments.

In all experiments, 60 min prior to construction of each agonist $E/[A]$ curve, a mixture of **cocaine** (30 μM), **timolol** (6 μM) and **SCH-23390** (R(+)-7-chloro-8-hydroxy-3-methyl-1-phenyl-2,3,4,5-tetrahydro-1H-3-benzazepine hydrochloride; 10 nM) were added to the KHS to block neuronal uptake, β₁/β₂-adrenoceptors and dopamine D₁ receptors respectively (Stam *et al.*, 1999).

Experimental design. In general, SMAs were exposed *in vitro* to single or combined challenges of noradrenaline and AVP in varying concentrations, with or without pretreatment with **phenoxybenzamine**, a non-selective

irreversible α -adrenoceptor blocker which also has a possible effect on calcium channels (Gengo *et al.*, 1984; McPherson *et al.*, 1985).

Interaction experiments without receptor inactivation. Concentration dependent contraction of rat SMA induced by noradrenaline or AVP in the absence or presence of the other drug was investigated according to the paired and single E/[A] curve protocols developed previously for noradrenaline (Stam *et al.*, 1999) and AVP (Stam *et al.*, 1998) respectively. Initial noradrenaline E/[A] curves were first obtained ($n = 19$) and were followed by 30 min washing and further equilibration for another 45 min. Subsequently, threshold contractions that amounted about 5, 10 or 25% of the maximum of the initial E/[A] curves were induced by AVP through increasing drug concentrations in small steps until desired contraction level was reached. After stabilization of the threshold contraction, second noradrenaline E/[A] curves were obtained. AVP E/[A] curves with no threshold contraction or with threshold contractions induced by noradrenaline that amounted about 5, 10 or 25% of the calibration contraction were obtained as described above but from separate vessel segments ($n = 18$).

Interaction experiments with prior receptor inactivation. In another set of experiments, the interaction between noradrenaline and AVP on the contraction of rat SMA was also assessed after pretreating the vessel segments with phenoxybenzamine. Prior to the interaction experiments, the vessel segments ($n = 8$) were pretreated with phenoxybenzamine (3 nM) for 5 min and were then washed eight times during a 30 min period and equilibrated for 45 min. Subsequently, the E/[A] curves of noradrenaline with or without a threshold contraction induced by AVP that amounted about 10% of the calibration contraction were produced as described earlier. Randomization and blinding were not applicable as this is not an intervention study.

Data analysis

Model development. Scaramellini and co-workers presented a theoretical 2R-1T model which provides a quantitative framework to interpret the interaction between two agonists, A_1 and A_2 , which bind to two different receptors, R_1 and R_2 , respectively, and produce a common intracellular mediator M leading to a pharmacological effect E (Figure 1)

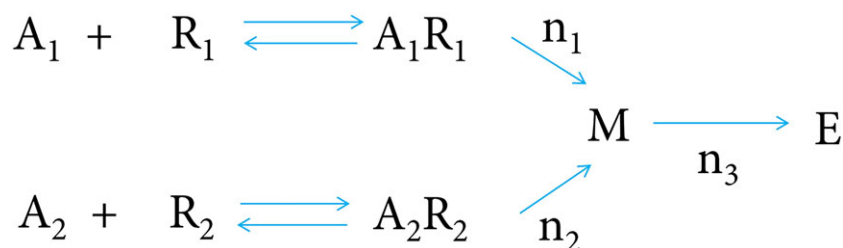


Figure 1

2R-1T model structure (Scaramellini *et al.*, 1997).

(Scaramellini *et al.*, 1997). For the current research, we analysed the experimental data of noradrenaline and AVP with the 2R-1T model. The estimation of model parameters and associated uncertainty/confidence intervals was based on simultaneous fitting of all individual data. The data and statistical analysis comply with the recommendations on experimental design and analysis in pharmacology (Curtis *et al.*, 2018).

The 2R-1T model assumes that the intracellular mediators $[M]_{NA}$ and $[M]_{AVP}$ amount depend on drug concentrations and have the algebraic form of a Hill equation (Equations 1 and 2). The pharmacological effect E is derived by $[M]_{Tot}$, the summation of mediator concentrations (Equation 3), also according to the Hill equation (Equation 4). Our experiments also included the addition of a third drug, phenoxybenzamine. To account for this inhibitor, two additional terms PBZ_A and PBZ_M were included (Equations 1 and 3), representing the irreversible blockade effect on α_{1A} -adrenoceptors and the inhibition effect on the common transducer respectively:

$$[M]_{NA} = \frac{m_{NA} \times PBZ_A \times [NA]^{n_{NA}}}{K_{NA}^{n_{NA}} + [NA]^{n_{NA}}} \quad (1)$$

$$[M]_{AVP} = \frac{m_{AVP} \times [AVP]^{n_{AVP}}}{K_{AVP}^{n_{AVP}} + [AVP]^{n_{AVP}}} \quad (2)$$

$$[M]_{Tot} = ([M]_{NA} + [M]_{AVP}) \times PBZ_M \quad (3)$$

Here, m_{NA} and m_{AVP} represent the maximum transducer amount that noradrenaline and AVP can produce, respectively and can be considered to represent receptor density, $[NA]$ and $[AVP]$ represent the concentrations of these two drugs, n_{NA} and n_{AVP} represent the Hill slope index of the two separated transduction pathways, K_{NA} and K_{AVP} represent the noradrenaline and AVP concentrations that produce half-maximal amount of $[M]_{NA}$ and $[M]_{AVP}$, which can be considered as the affinities of noradrenaline and AVP on α_{1A} -adrenoceptors and V_{1A} receptors respectively. We considered both estimating K_{NA} and K_{AVP} , and fixing these parameters to the published values, identified as 4.27 μ M (Nyborg and Bevan, 1988) and 0.24 nM (Bockman *et al.*, 1992) respectively. PBZ_A and PBZ_M were both constrained to values between 0 and 1. In the absence of phenoxybenzamine, PBZ_A and PBZ_M were both set to be 1 as the receptor or transducer

is intact. Finally, the $E/[A]$ relationship for noradrenaline and AVP was characterized with Equation 4:

$$E = \frac{E_{max} \times [M]_{tot}^{n_M}}{K^{n_M} + [M]_{tot}^{n_M}} \quad (4)$$

Here, E_{max} represents the maximum possible system effect, K represents the amount of $[M]_{tot}$ at half-maximal value of E , and n_M represents the Hill slope index of the common transduction pathway. The absolute value of K is unidentifiable, and was therefore fixed to 1, which means both numerator and denominator of Equation 4 were divided by K . Thus, the estimates of m_{NA} and m_{AVP} could be expressed as m_{NA}/K and m_{AVP}/K .

A mixed-effect modelling approach was applied to account for inter-individual variability (IIV). Parameter estimate was performed through the first order conditional estimation method with interaction (FOCEI), implemented in nonlinear mixed-effect modelling software NONMEM, version 7.3.0 (ICON Development Solutions) (Keizer *et al.*, 2013). IIV was estimated for m_{NA}/K , m_{AVP}/K and E_{max} with Equation 5, where P_i represents the parameter of each experiment, P_{tp} represents typical value of the parameter, and η represents the IIV which was assumed to be log-normally distributed with mean of 0 and variance of ω^2 . IIV of K_{NA} and K_{AVP} were also estimated while fixing the corresponding typical values as literature values. Residual error was characterized with additive error model with Equation 6, where $Y_{obs,i}$ represents observations, $Y_{pred,i}$ represents predictions, and ε represents the residual error which was also assumed to log-normally distributed with mean of 0 and variance of σ^2 .

$$P_i = P_{tp} \times e^{\eta_i} \quad (5)$$

$$Y_{obs,i} = Y_{pred,i} + \varepsilon_i \quad (6)$$

Precision of parameter estimates, which was reflected by relative standard error (RSE) of parameters, and the Akaike information criterion (AIC) were regarded as the criteria to assess the goodness-of-fit (GOF) of model. Standard GOF plots and a visual predictive check (VPC) were also used to assess the model performance (N Nguyen *et al.*, 2017).

Translation to human contractile data. We investigated the extrapolation of the model to human data by adjusting parameters m_{NA}/K and m_{AVP}/K according to the difference in receptor density of α_{1A} -adrenoceptors and V_{1A} receptors between rat and human vessels (Eq. 7), while K_{NA} and K_{AVP} were kept unchanged:

$$P_H = P_R \times \frac{C_H}{C_R} \quad (7)$$

Here, P_H and P_R represent parameter m_{NA}/K and m_{AVP}/K for human and rat respectively, and C_H and C_R respectively represent the receptor density in human and rat vessels. C_H and C_R were reported respectively as 61.6 fmol·mg⁻¹ of protein (Yamada *et al.*, 1994) and 101 fmol·mg⁻¹ of protein (Faber *et al.*, 2001) for α_{1A} -adrenoceptors and 36 fmol·mg⁻¹ of protein (Serradeil-Le Gal *et al.*, 1995) and 52 fmol·mg⁻¹ of protein (Vågnes *et al.*, 2004) for V_{1A} receptors, making the ratio

C_H/C_R 0.61 and 0.69 for α_{1A} -adrenoceptors and V_{1A} receptors respectively.

Drug induced $E/[A]$ curves in human were derived from published data where human renal arterial rings were challenged *ex vivo* with noradrenaline with or without small concentrations of AVP (0.1 and 0.03 nM) (Segarra *et al.*, 2002). The data points were digitized by WebPlotDigitizer, version 3.11 (<http://arohatgi.info/WebPlotDigitizer/app/>). The scaled model performance was assessed by comparing the result of 500 simulations with observed human data. The predictive performance of the model without any scaling for receptor density was also assessed as a comparison.

Contractile responses in the human study were expressed relative to a response to 100 mM KCl, the relative level of which differs from that of the calibration contraction (i.e. the response to 10 μ M noradrenaline) used in our rat experiment. Therefore, to make the scaled model predictions be comparable with the human data, the simulation results were adjusted through being multiplied by the human contraction response induced by 10 μ M noradrenaline, which was 150% of the response to 100 mM KCl.

Sensitivity analysis was performed to evaluate the effects of receptor density ratios and drug affinity values on the scaled model predictions respectively. The C_H/C_R ratio of α_{1A} -adrenoceptors and V_{1A} receptors as well as K_{NA} and K_{AVP} were set as 0.5-fold, onefold and twofold of the original values, respectively, and the prediction results were assessed by plotting population prediction results together with the human experimental data where human vessels were challenged with noradrenaline and 0.1 nM of AVP.

Materials

[Arg⁸] vasopressin, cocaine hydrochloride, methacholine bromide, l-noradrenaline hydrochloride, phenoxybenzamine hydrochloride and timolol maleate were purchased from Sigma, Zwijndrecht, the Netherlands. SCH 23390 were purchased from Research Biochemicals Incorporated, Natick, USA. Noradrenaline was dissolved in stoichiometric ascorbic acid solution. Methacholine and phenoxybenzamine were dissolved in ethanol, and the final amount of ethanol in organ bath was <1% which causes no extra relaxation on the vessel segments (Ru *et al.*, 2008). All other drugs were dissolved in distilled water.

Nomenclature of targets and ligands

Key protein targets and ligands in this article are hyperlinked to corresponding entries in <http://www.guidetopharmacology.org>, the common portal for data from the IUPHAR/BPS Guide to PHARMACOLOGY (Harding *et al.*, 2018), and are permanently archived in the Concise Guide to PHARMACOLOGY 2017/18 (Alexander *et al.*, 2017).

Results

Effects of noradrenaline, AVP and phenoxybenzamine on contraction

Noradrenaline caused concentration-dependent contractions of SMAs (Figure 2A). Individual $E/[A]$ curves were fitted to the Hill equation as described in Stam *et al.* (1998, 1999) to obtain estimates of midpoint location ($pEC_{50} = -\log(EC_{50})$)

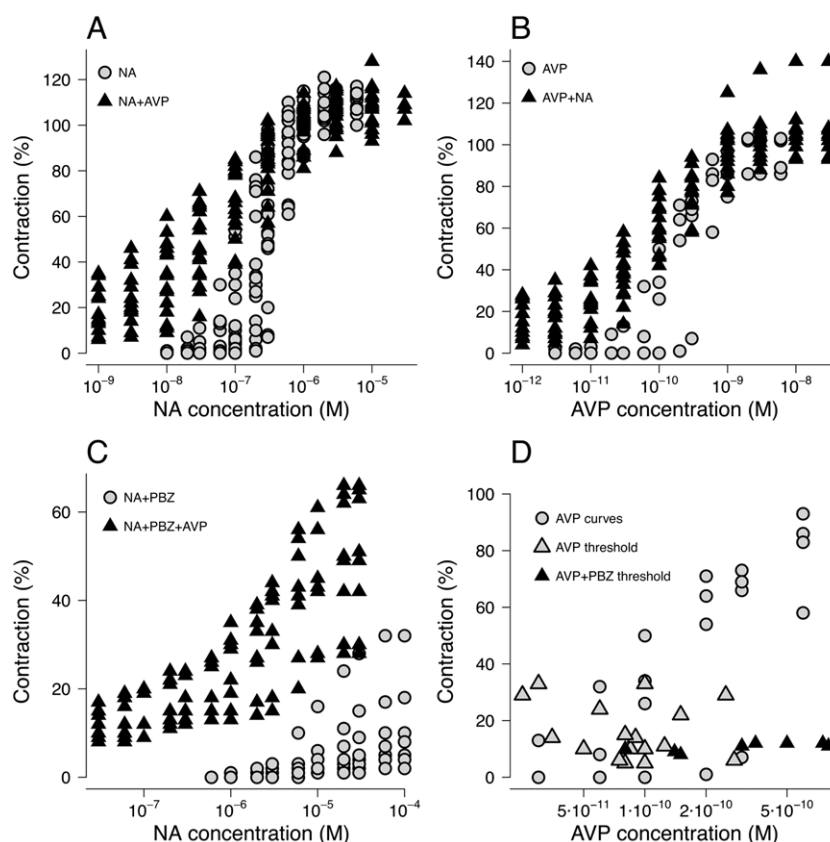


Figure 2

Concentration dependent contraction curves induced by (A) noradrenaline (NA) in the absence of AVP ($n = 19$) and presence of AVP ($n = 19$, concentration range from 0.025 to 0.275 nM); (B) AVP with absence of noradrenaline ($n = 4$) and presence of noradrenaline ($n = 14$, concentration range from 30 to 280 nM); and (C) noradrenaline with absence of AVP ($n = 8$) and presence of AVP ($n = 8$, concentration range from 0.08 to 0.8 nM) while 3 nM phenoxybenzamine (PBZ) was present. (D) E/[A] curves induced by AVP without thresholds ($n = 4$) and the threshold contractions induced by AVP without ($n = 14$) or with ($n = 8$) pretreatment with 3 nM phenoxybenzamine. When phenoxybenzamine was present, higher AVP concentration was needed to reach the same contraction level as when phenoxybenzamine was absent. Responses were expressed as percentages of the contraction induced by the fifth previous noradrenaline (10 μ M) challenge.

and Hill slope (n_H). Threshold contractions that amounted to $5.5 \pm 0.6\%$ (mean \pm SD, $n = 4$), $12.4 \pm 2.3\%$ ($n = 8$) and $28.4 \pm 4.2\%$ ($n = 7$) of the calibration contraction were induced by 0.13 ± 0.1 , 0.08 ± 0.03 and 0.09 ± 0.08 nM AVP respectively. The three threshold contractions to AVP caused a >twofold flattening of the control noradrenaline E/[A] curves [n_H changed from 2.67 ± 0.67 ($n = 19$) to 1.04 ± 0.17 , 0.81 ± 0.10 and 0.75 ± 0.06 , respectively], and a leftward shift of up to ~fourfold (pEC_{50} changed from 6.57 ± 0.23 to 6.89 ± 0.29 , 7.16 ± 0.32 and 7.15 ± 0.38 , respectively), without changing the maximum response (Figure 2A).

AVP also caused concentration-dependent contractions of SMAs (Figure 2B). Pre-incubating with 0.07 ± 0.05 ($n = 4$), 0.08 ± 0.03 ($n = 5$) and 0.21 ± 0.08 ($n = 5$) μ M noradrenaline produced threshold contractions that amounted to 6.0 ± 2.2 , 11.2 ± 1.6 and $24.0 \pm 3.2\%$ of the calibration contraction respectively. The three threshold contractions to noradrenaline also caused a >twofold flattening of the AVP E/[A] curves compared to control [n_H changed from 2.31 ± 1.4 ($n = 4$) to 1.08 ± 0.17 , 0.85 ± 0.17 and 0.83 ± 0.08 , respectively], and a leftward shift of up to ~3.5-fold (pEC_{50} changed from 9.71 ± 0.32 to 9.96 ± 0.18 , 10.22 ± 0.26 and 9.87 ± 0.28 ,

respectively), without changing the maximum response (Figure 2B). The reported n numbers were used only for data display and calculation of SD and not for any statistical comparison.

Pretreating with phenoxybenzamine reduced the maximum noradrenaline-induced contraction from 111 ± 4.8 to $10 \pm 10.3\%$ ($n = 8$) and caused a rightward shift of the noradrenaline E/[A] curves (Figure 2C). When AVP was added, the noradrenaline E/[A] curves were potentiated and flattened with maximum contraction increased to $49 \pm 15.1\%$ ($n = 8$) (Figure 2C).

In addition to the well-established inhibitory effect of phenoxybenzamine on noradrenaline (Van der Graaf and Stam, 1999), when plotting AVP-induced E/[A] curves together with AVP-induced threshold contractions with or without presence of phenoxybenzamine, the combination of AVP with phenoxybenzamine also appeared to be associated with an inhibitory effect (Figure 2D).

Model development and evaluation

In their theoretical paper, Scaramellini *et al.* (1997) demonstrate that the 2R-1T model predicts a variety of patterns of

agonist E/[A]-curve location and slope changes induced by the presence of another agonist. Our data (leftward shift, flattening and no change in maximum response) are entirely consistent with the scenario for two full agonists which share a common transduction pathway with a steep slope. We therefore developed our further analysis of the data on the basis of this 2R-1T model framework.

The parameter estimates obtained after fitting the experimental data to the 2R-1T model are shown in Table 1. Two models were considered. In Model 1, all parameters were estimated but the RSEs of m_{AVP}/K and K_{AVP} were >100%, indicating that the information our experimental data provided could not support precise estimation of these parameters. Nonetheless, K_{NA} could be estimated with better precision (RSE = 26%) and was close to the previously reported values (Nyborg and Bevan, 1988). Other parameters were estimated with acceptable precision (RSE < 25%). After fixing the typical value of K_{NA} and K_{AVP} to published values while estimating corresponding IIV (Model 2), all model parameters could be estimated with greater precision (RSE ≤ 20%). The AIC of Model 2 was 3777 and was 22 lower than that of Model 1, which was 3799, indicating that Model 2 had better GOF than Model 1. Therefore, the model with fixed K_{NA} and K_{AVP} was selected to characterize our experimental dataset. Model evaluation results of Model 2 are shown in Figures 3 and 4. Both population predictions and individual predictions were comparable to the observations (Figure 3A, B), and no trends were observed in the conditional weighted residuals (Figure 3C). The VPC plots (Figure 4), where model simulations were plotted together with observed data points for different dose regimens, showed that most observations could be adequately covered within the 97.5th and 2.5th percentiles of model simulations, and the 50th percentiles of observations could mostly fit within the 95% confidence intervals of the 50th percentiles of

simulations, although wider simulation confidence intervals were shown in Figure 4C, E, F due to the fewer curves involved in the corresponding scenarios. Using the developed model, the interactions between noradrenaline and AVP concentrations on contraction can be visualized using a response surface plot (Figure 5).

The extent of phenoxybenzamine inhibitory effects were also estimated in the model. It was identified that the addition of 3 nM phenoxybenzamine reduced the noradrenaline-induced contractions by 92.6% and reduced AVP-induced contractions by 44.3%.

Prediction of the contractile response of human vessels

According to the simulation results, the model derived from rat experimental data could not successfully capture experimental data for human renal arteries assuming a 1–1 cross-species translation with identical parameters (Figure 6A, B). However, after adjusting m_{NA}/K and m_{AVP}/K by accounting for the differences in receptor density between species, human data were shown to be adequately described by the model (Figure 6C, D).

The results of sensitivity analysis showed that compared with changing drug affinity values, a change in receptor density ratio appeared to have a greater overall effect on 2R-1T model scaling results. Half reduction or a twofold increase of original α_{1A} -adrenoceptor C_H/C_R ratio, as well as a twofold increase of original V_{1A} receptor C_H/C_R ratio resulted in apparently inferior prediction of human data (Figure 7), while half reduction of original V_{1A} receptor C_H/C_R ratio only slightly changed the accuracy of predictions. In contrast, halving original K_{NA} or K_{AVP} values resulted in less accurate predictions, while doubling original K_{NA} or K_{AVP} values affected the scaling results less (Figure 8).

Table 1

Parameter estimates of the model where K_{NA} and K_{AVP} were not fixed (Model 1) and where K_{NA} and K_{AVP} were fixed (Model 2)

Parameter	Model 1			Model 2		
	Estimates	RSE%	IIV (CV%)	Estimates	RSE%	IIV (CV%)
m_{NA}/K (–)	8.35	13.2	34.8	7.56	8.3	25.5
n_{NA} (–)	0.658	4.7	–	0.665	3.8	–
m_{AVP}/K (–)	8.59	189.8	44.3	1.75	6.9	27.0
n_{AVP} (–)	0.495	14.5	–	0.690	7.1	–
K_{NA} (10^{-6} M)	5.65	26.4	–	4.27 FIX	–	51.6
K_{AVP} (10^{-9} M)	18.1	478.5	–	0.24 FIX	–	91.2
E_{max} (%)	105	2.0	9.0	108	1.4	8.0
n_M (–)	3.77	5.4	–	3.75	5.3	–
PBZ_A	0.120	24.1	–	0.132	20.4	–
PBZ_M	0.585	14.9	–	0.557	11.6	–
Residual errors						
ADD (SD, %)	4.66	–	–	4.53	–	–

ADD, additive error; CV, coefficient of variation; IIV, inter-individual variability.

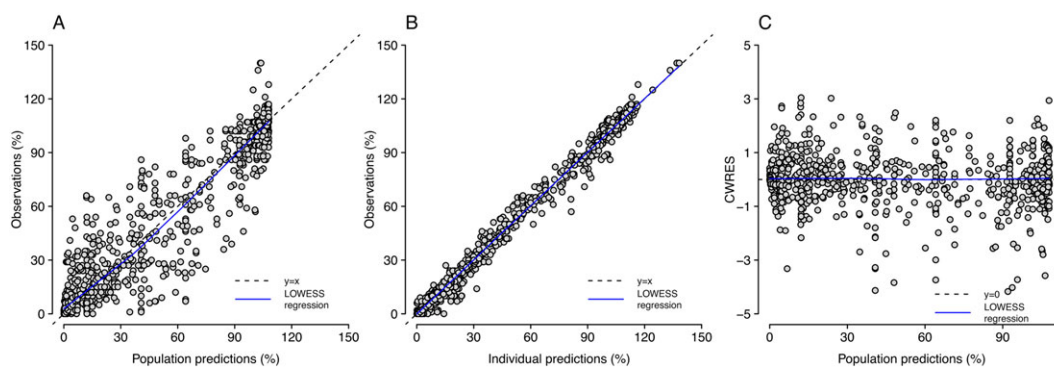


Figure 3

GOF plots for the final model, including observations versus population predictions (A), observations versus individual predictions (B), and conditional weighted residual errors (CWRES) versus population predictions (C). Locally weighted scatterplot smoothing (LOWESS) regression lines were also plotted.

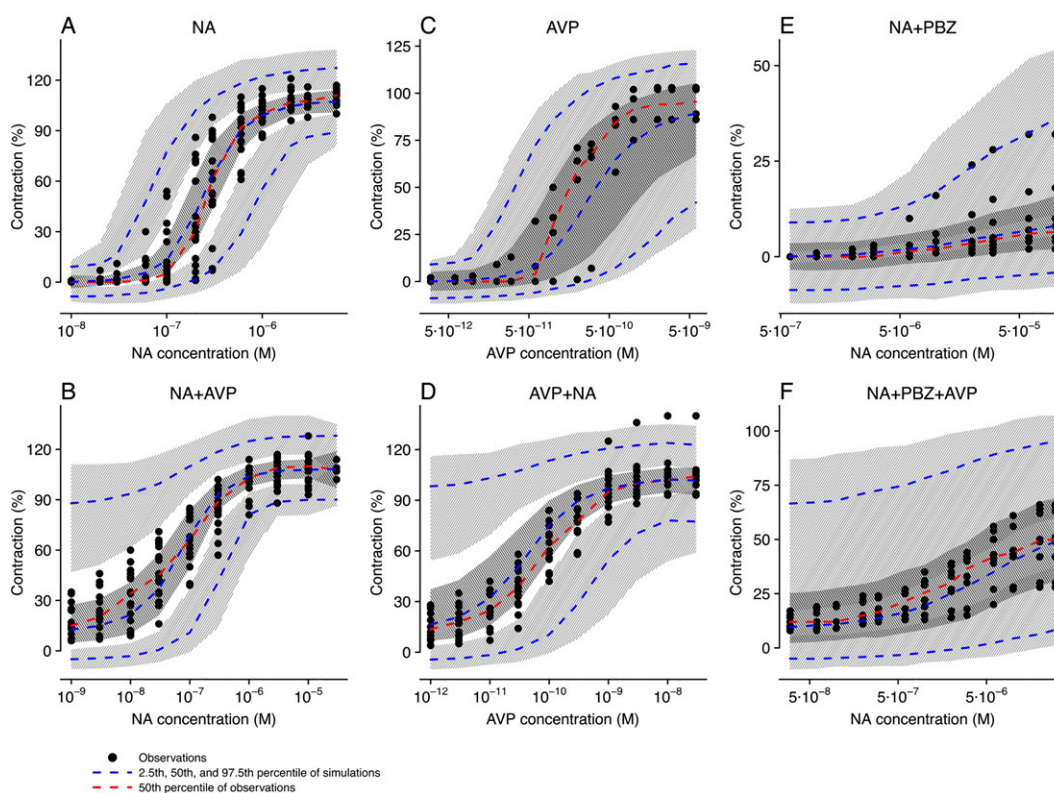


Figure 4

Visual predictive check of the final model stratified on different dose regimens: (A) noradrenaline (NA) only; (B) noradrenaline with fixed concentrations of AVP; (C) AVP only; (D) AVP with fixed concentrations of noradrenaline; (E) noradrenaline only when phenoxybenzamine (PBZ) was added; (F) noradrenaline with fixed concentrations of AVP when phenoxybenzamine was added. Light grey hatching represents 95% confidence interval of the 2.5th and 97.5th percentile of simulations, and dark grey hatching represents 95% confidence interval of the 50th percentile of simulations.

Discussion

The previously proposed 2R-1T model provides an attractive quantitative framework to characterize drug–drug interactions in a mechanism-based fashion. Unlike other commonly used mechanism-based modelling methodologies (Koch *et al.*, 2016), the 2R-1T model allows the description of the interaction between two agonists acting on different receptors.

Meanwhile, in comparison with fully mechanistic ordinary differential equation models that concern complex receptor bindings and underlying signalling pathways (Bianconi *et al.*, 2012), the 2R-1T model is simpler to be implemented as less prior knowledge is required. In this study, we have shown that this model can indeed be used to successfully describe the interaction between two agonists of interest that share a common transduction pathway and scale to human,

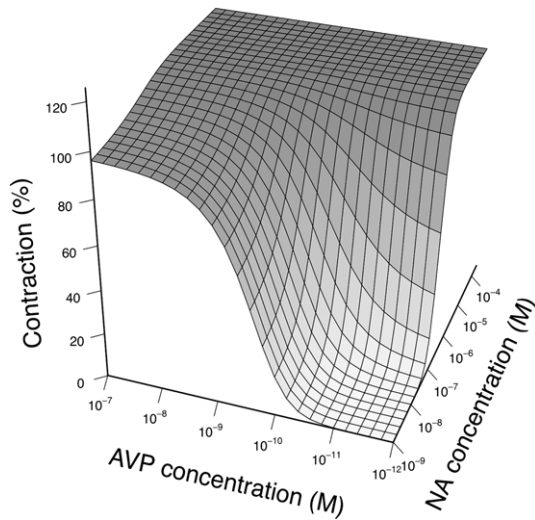


Figure 5

Response surface plot for the predicted contraction of different combinations of noradrenaline (NA) and AVP as predicted by the developed 2R-1T model.

using a case example for contractile responses induced by noradrenaline and AVP.

The 2R-1T model structure assumes the combination effect was derived by the summation of mediator concentrations, which matches the pharmacological mechanisms of noradrenaline and AVP-induced vasoconstriction. The estimates of m_{NA}/K and m_{AVP}/K were much larger than 1, indicating that the concentrations of transducer ($[M]_{NA}$ and $[M]_{AVP}$) produced by noradrenaline or AVP are able to reach saturation of the E/[A] curves. This is consistent with the fact that although the contractions of rat SMA induced by noradrenaline and AVP were mutually potentiated, the maximum effects (E_{max}) induced by either drug alone or in combination were similar (Figure 2). Estimates of n_{NA} and n_{AVP} indicated that the slope of transducer production for noradrenaline and AVP was similar. The slope change of noradrenaline or AVP E/[A] curves that occurred when the other drug produced a certain level of threshold could be captured by the estimate of n_M , as was shown in the simulation results of the initial theoretical model (Scaramellini *et al.*, 1997).

As there is no irreversible antagonist available for V_{1A} receptors (Lolait *et al.*, 2018), the E/[A] curves required to estimate K_{AVP} and m_{AVP}/K were not obtained, which was

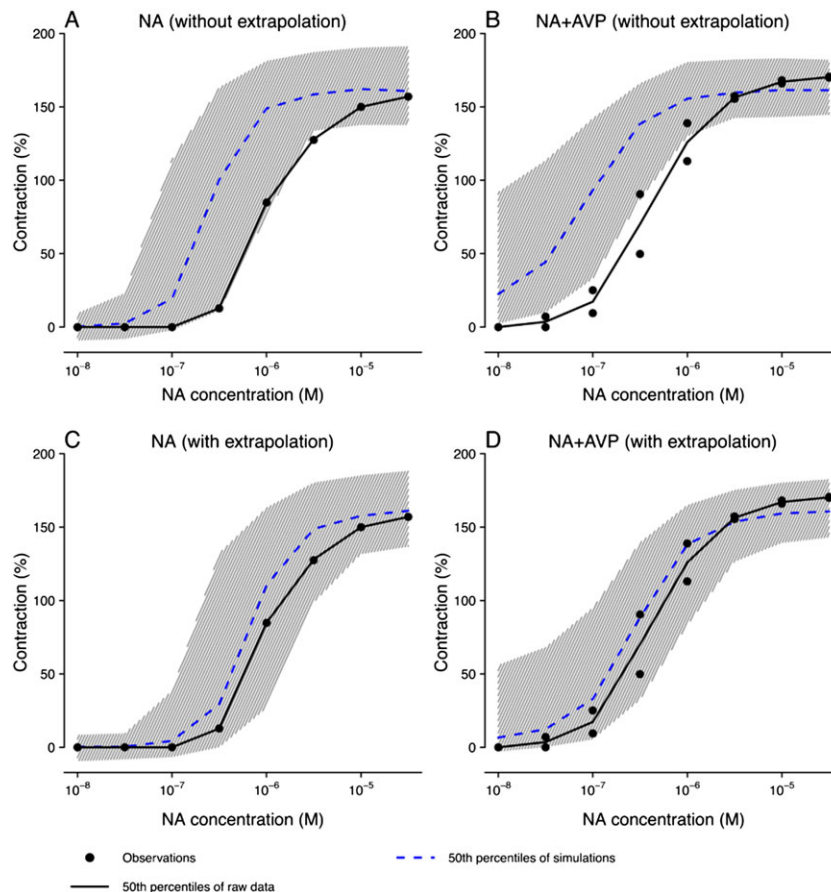


Figure 6

Prediction of human vasoconstriction data under challenging with noradrenaline (NA) only (A and C) and noradrenaline with two different concentrations of AVP (0.1 and 0.03 nM) (B and D), based on the model without extrapolation (A and B) and with scaled receptor capacities, where the scaling term on m_{NA}/K and m_{AVP}/K were 0.61 and 0.69 respectively (C and D). Grey hatching represents 95% confidence interval of the 50th percentile of simulations.

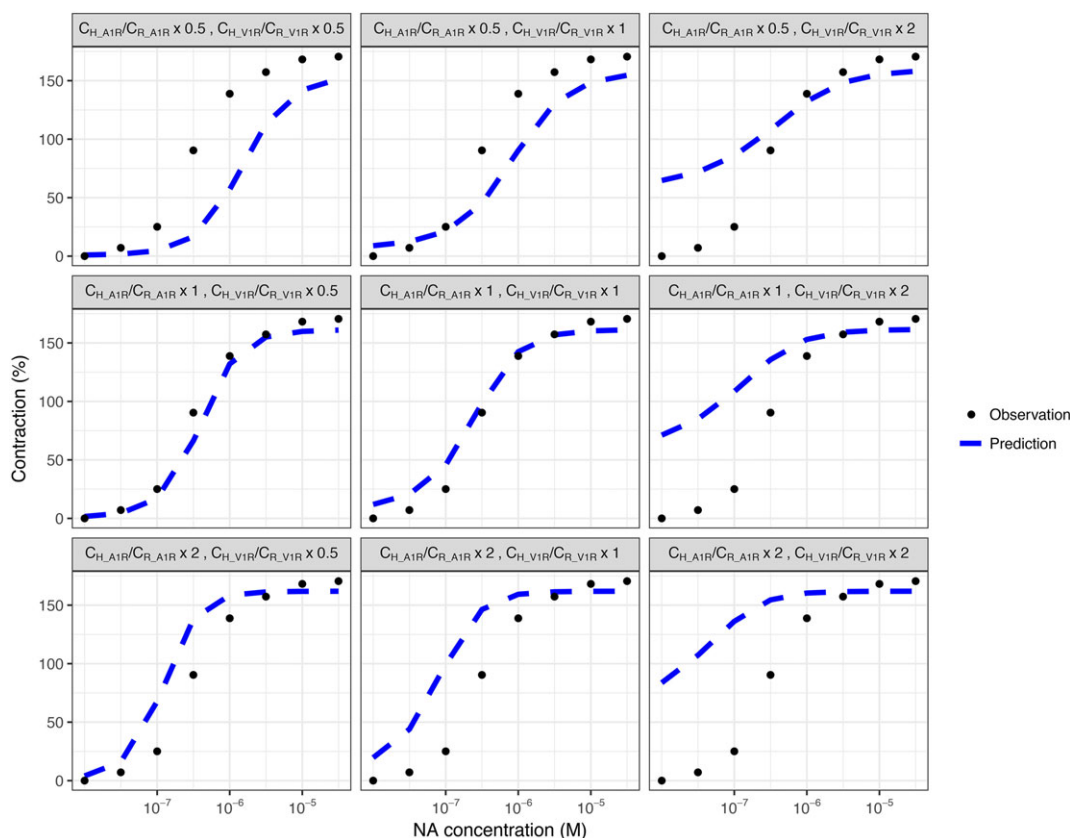


Figure 7

Sensitivity analysis for evaluating the effects of receptor density ratios (C_H/C_R) on the scaled model predictions. The C_H/C_R ratio of α_{1A} -adrenoceptors and V_{1A} receptors were set as 0.5-fold, onefold and twofold of the original using values. Population predictions were plotted together with the human experimental data where human vessels were challenged with noradrenaline (NA) and 0.1 nM of AVP.

considered to be the main reason why K_{AVP} (RSE = 478.5%) and m_{AVP}/K (RSE = 189.8%) could not be estimated with acceptable accuracy (Table 1, Model 1). Therefore, the value of K_{NA} and K_{AVP} was ultimately fixed according to published values. The reported value of K_{NA} in rat SMA was identified as 0.66–4.27 μ M (Nyborg and Bevan, 1988; Oriowo *et al.*, 1989; Van der Graaf and Stam, 1999) and that of K_{AVP} was identified as 0.16–1.25 nM (Lariviere *et al.*, 1989, 1988; Gopalakrishnan *et al.*, 1991; Bockman *et al.*, 1992). Besides the values we applied, using other identified values to fit the data showed to have inferior GOF results (AIC increased by 1 to 114). Therefore, the values of K_{NA} and K_{AVP} were finally set as 4.27 μ M (Nyborg and Bevan, 1988) and 0.24 nM (Bockman *et al.*, 1992), respectively, to fit our experimental data.

The use of a mixed-effect model was of particular relevance to account for the IIV of the data as it may lead to bias in parameter estimates if the variance between individual vessel segments were not considered appropriately. The IIV of the maximum effect was small, while for m_{NA}/K , m_{AVP}/K , K_{NA} and K_{AVP} it was more pronounced, which was considered to primarily account for the variability among observations. The IIV of PBZ_A and PBZ_M was too small to be identified, thus they were not included in our model. This population analysis approach also allowed us to analyse all individual data simultaneously which dealt with the unequal number of

$E/[A]$ curves for noradrenaline and AVP result from the paired and single curve protocols effectively.

The effect of phenoxybenzamine was characterized by two independent terms, which respectively refers to (i) the inactivation effect on α_{1A} -adrenoceptors and (ii) the inhibition effect on the common signal transducer for both noradrenaline and AVP stimulus to account for phenoxybenzamine caused contraction decrease for both noradrenaline and AVP. This is in accordance with the underlying mechanism that phenoxybenzamine as a non-selective irreversible α -adrenoceptor blocker has well-established inhibitory effect on noradrenaline through α_{1A} -adrenoceptors (Van der Graaf and Stam, 1999), and phenoxybenzamine was also reported previously to have an inhibition effect on calcium channels (Gengo *et al.*, 1984; McPherson *et al.*, 1985) and calmodulin (Conant *et al.*, 2003). These latter mechanisms were considered to contribute to phenoxybenzamine inhibition of AVP-induced contraction shown in Figure 2D as well as on noradrenaline, as calcium is a common signal transducer of noradrenaline and AVP (Mauger *et al.*, 1984). This current approach resulted in a significantly better fit of the overall data (AIC decreased 8.7) comparing with only using one term to describe the effect of phenoxybenzamine. The results shown in GOF and VPC plots confirmed the satisfactory fit and predictive performance of our model.

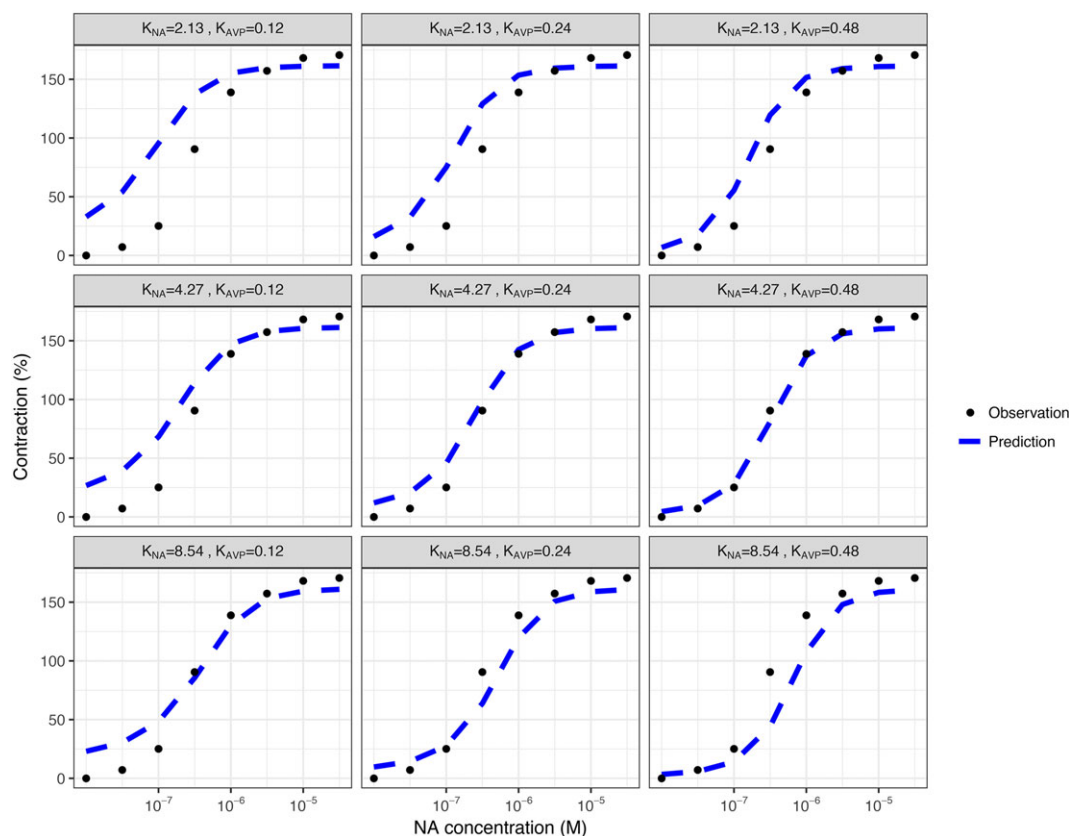


Figure 8

Sensitivity analysis for evaluating the effects of drug affinity values on the scaled model predictions. The K_{NA} and K_{AVP} were set as 0.5-fold, onefold and twofold of the original using values. Population predictions were plotted together with the human experimental data where human vessels were challenged with noradrenaline (NA) and 0.1 nM of AVP.

The main limitation of our study is inherent to the *in vitro* assay system used and the fact that measurements were only obtained at (pseudo) steady-state conditions, which does not take into account the role of time-dependent changes in pharmacokinetics and pharmacodynamics and feedback mechanisms present in intact *in vivo* models. In addition, receptor binding kinetics (de Witte *et al.*, 2016) and receptor turnover (Dua *et al.*, 2015) were not considered in the current 2R-1T model, because no evidence was observed for slow-onset or (de)sensitization of the effect (Van der Graaf *et al.*, 1996; Stam *et al.*, 1999, 1998; Van der Graaf and Stam, 1999). Also, we did not explore the effect of repeated dosing in the current study. Of course, such mechanistic elements could be added when new data emerges that underpin the development of more advanced versions of the 2R-1T model.

We further demonstrated that the 2R-1T model allows inter-species extrapolation from rat to humans, indicating that our approach can be applied in translational research. The initial significant discrepancy between observed human data and the corresponding predictions from the model without scaling, which assumed identical parameters for rat and human, suggested an important pharmacological difference between species. Relative differences in receptor density of blood vessels and drug affinities were

considered to be the most likely causes of this difference. The reported range of noradrenaline and AVP affinity for α_{1A} -adrenoceptors and V_{1A} receptors were from 0.40–1.58 μ M (Perez *et al.*, 2018) and 0.50–3.16 nM (Lolait *et al.*, 2018) respectively in humans and from 0.66–4.27 μ M and 0.16–1.25 nM respectively in rats. As the ranges of affinity values for human and rats overlap, K_{NA} and K_{AVP} were kept unchanged during scaling. Receptor density values, which were demonstrated to have greater influence on the inter-species scaling of 2R-1T model from sensitivity analysis, were derived from previous reports where the studies were mostly performed on aortic tissue, which was the closest related tissue where we could identify density data. An additional suitable receptor density value for V_{1A} receptors was also identified as 325 $\text{fmol}\cdot\text{mg}^{-1}$ of protein for five 8-week-old rats and 45 $\text{fmol}\cdot\text{mg}^{-1}$ of protein for four 12-week-old rats (Lariviere *et al.*, 1989), the mean of which is 201 $\text{fmol}\cdot\text{mg}^{-1}$ of protein. When applying this mean value, the model scaling results did not change dramatically, as shown by the sensitivity analysis that the reduction of the V_{1A} receptor C_H/C_R ratio did not greatly affect the accuracy of scaling model predictions. On the basis of our current finding, the potential clinical value of this model structure on scaling from adults to paediatrics based on age-dependent expression of α_{1A} -adrenoceptors

and V_{1A} receptors could be further investigated. The applicability of such a system–pharmacology approach to explaining differences between hERG-mediated QTC prolongation in adults and neonates on the basis of model-predicted differences in target expression levels, which were consistent with experimentally derived mRNA levels in patients (Moric-Janiszewska *et al.*, 2011), has been recently demonstrated (Gotta *et al.*, 2016).

In conclusion, we have shown, for the first time, that the 2R-1T model can be applied to characterize the interaction between two clinically relevant agonists acting at different receptors but producing effects through a converging transduction pathway. Our data (leftward shift, flattening and no change in maximum response) are entirely consistent with the theoretical predictions made by Scaramellini *et al.* (1997) for two full agonists which share a common transduction pathway with a steep slope. As pointed out by these authors, their 2R-1T model may not be universally applicable and is undoubtedly an oversimplification of receptor transduction pathways, but our first experimental validation provided support for its validity. We therefore propose that this simple quantitative systems pharmacology model structure provides a translational framework to mechanistically interpret and predict drug–drug interactions and is of significant value to rationally optimize novel combination treatments. We believe this is fully in line with the new 2017 European Medicines Agency guideline on nonclinical and clinical aspects of first-in-human (FIH) and early clinical trials, which puts more emphasis on the better use of preclinical data to guide rational dose selection of FIH studies (Ponzano *et al.*, 2018; Van der Graaf and Benson, 2018).

Acknowledgements

This work was supported by the IMI TransQST consortium. We also would like to thank Dr Viji Chelliah (Certara QSP) for help with receptor expression data mining.

Author contributions

All authors contributed to manuscript writing. An.Y. and Ak.Y. performed the data analysis. W.B.S. and P.v.d.G. designed and performed the experiments. J.G.C.v.H. and P.v.d.G. supervised this work.

Conflict of interest

The authors declare no conflicts of interest.

Declaration of transparency and scientific rigour

This Declaration acknowledges that this paper adheres to the principles for transparent reporting and scientific rigour of preclinical research recommended by funding agencies, publishers and other organisations engaged with supporting research.

References

- Al-Lazikani B, Banerji U, Workman P (2012). Combinatorial drug therapy for cancer in the post-genomic era. *Nat Biotechnol* 30: 679–692.
- Alexander SPH, Christopoulos A, Davenport AP, Kelly E, Marrion NV, Peters JA *et al.* (2017). The Concise Guide to PHARMACOLOGY 2017/18: G protein-coupled receptors. *Br J Pharmacol* 174: S17–S129.
- Bianconi F, Baldelli E, Ludovini V, Crinò L, Flacco A, Valigi P (2012). Computational model of EGFR and IGF1R pathways in lung cancer: a systems biology approach for translational oncology. *Biotechnol Adv* 30: 142–153.
- Bockman CS, Jeffries WB, Pettinger WA, Abel PW (1992). Reduced contractile sensitivity and vasopressin receptor DOCA-salt hypertension. *Am J Physiol* 262: H1752–H1758.
- Christ GJ, Jean-Jacques M (1991). Mutual-effect amplification of contractile responses elicited by simultaneous activation of α -1 adrenergic and 5-hydroxytryptamine₂ receptors in isolated rat aorta. *J Pharmacol Exp Ther* 256: 553–561.
- Cohen ML, Schenck K (2000). Contractile responses to sumatriptan and ergotamine in the rabbit saphenous vein: effect of selective 5-HT_{1F} receptor agonists and PGF 2 α . *Br J Pharmacol* 131: 562–568.
- Conant AR, Shackcloth MJ, Oo AY, Chester MR, Simpson AWM, Dihmis WC (2003). Phenoxybenzamine treatment is insufficient to prevent spasm in the radial artery: the effect of other vasodilators. *J Thorac Cardiovasc Surg* 126: 448–454.
- Curtis MJ, Alexander S, Cirino G, Docherty JR, George CH, Giembycz MA *et al.* (2018). Experimental design and analysis and their reporting II: updated and simplified guidance for authors and peer reviewers. *Brit J Pharmacol* 175: 987–993.
- Danhof M, de Jongh J, De Lange ECM, Della Pasqua O, Ploeger BA, Voskuyl RA (2007). Mechanism-based pharmacokinetic-pharmacodynamic modeling: biophase distribution, receptor theory, and dynamical systems analysis. *Annu Rev Pharmacol Toxicol* 47: 357–400.
- de Witte WEA, Danhof M, van der Graaf PH, de Lange ECM (2016). In vivo target residence time and kinetic selectivity: the association rate constant as determinant. *Trends Pharmacol Sci* 37: 831–842.
- Dellinger RP, Levy MM, Rhodes A, Annane D, Gerlach H, Opal SM *et al.* (2013). Surviving sepsis campaign: international guidelines for management of severe sepsis and septic shock, 2012. *Intensive Care Med* 39: 165–228.
- Dua P, Hawkins E, and van der Graaf PH (2015). A tutorial on target-mediated drug disposition (TMDD) models 324–337.
- Faber JE, Yang N, Xin X (2001). Expression of α -adrenoceptor subtypes by smooth muscle cells and adventitial fibroblasts in rat aorta and in cell culture. *J Pharmacol Exp Ther* 298: 441–452.
- Fitzgerald JB, Schoeberl B, Nielsen UB, Sorger PK (2006). Systems biology and combination therapy in the quest for clinical efficacy. *Nat Chem Biol* 2: 458–466.
- Gabrielsson J, Gibbons FD, Peletier LA (2016). Mixture dynamics: combination therapy in oncology. *Eur J Pharm Sci* 88: 132–146.
- Gengo PJ, Yousif F, Janis RA, Triggler DJ (1984). Interaction of phenoxybenzamine with muscarinic receptors and calcium channels. *Biochem Pharmacol* 33: 3445–3449.

- Gerthoffer WT (1996). Agonist synergism in airway smooth muscle contraction. *J Pharmacol Exp Ther* 278: 800–807.
- Gopalakrishnan V, Xu YJ, Sulakhe PV, Triggler CR, McNeill JR (1991). Vasopressin (V1) receptor characteristics in rat aortic smooth muscle cells. *Am J Physiol* 261: H1927–H1936.
- Gotta V, Yu Z, Cools F, van Ammel K, Gallacher DJ, Visser SAG *et al.* (2016). Application of a systems pharmacology model for translational prediction of hERG-mediated QTc prolongation. *Pharmacol Res Perspect* 4: e00270.
- Harding SD, Sharman JL, Faccenda E, Southan C, Pawson AJ, Ireland S *et al.* (2018). The IUPHAR/BPS Guide to PHARMACOLOGY in 2018: Updates and expansion to encompass the new guide to IMMUNOPHARMACOLOGY. *Nucleic Acids Res* 46: D1091–D1106.
- Jonker DM, Visser SAG, Van der Graaf PH, Voskuyl RA, Danhof M (2005). Towards a mechanism-based analysis of pharmacodynamic drug-drug interactions in vivo. *Pharmacol Ther* 106: 1–18.
- Keizer RJ, Karlsson MO, Hooker A (2013). Modeling and simulation workbench for NONMEM: tutorial on Pirana, PsN, and Xpose. *CPT Pharmacometrics Syst Pharmacol* 2: 1–9.
- Kilkenny C, Browne W, Cuthill IC, Emerson M, Altman DG (2010). Animal research: reporting in vivo experiments: the ARRIVE guidelines. *Br J Pharmacol* 160: 1577–1579.
- Koch G, Schropp J, Jusko WJ (2016). Assessment of non-linear combination effect terms for drug–drug interactions. *J Pharmacokinet Pharmacodyn* 43: 461–479.
- Lariviere R, Baribeau J, St-Louis J, Schiffrin EL (1989). Vasopressin receptors and inositol trisphosphate production in blood vessels of spontaneously hypertensive rats. *Can J Physiol Pharmacol* 67: 232–239.
- Lariviere R, St-Louis J, Schiffrin EL (1988). Vascular binding sites and biological activity of vasopressin in doca-salt hypertensive rats. *J Hypertension* 6: 211–217.
- Leff P (1987). An analysis of amplifying and potentiating interactions between agonists. *J Pharmacol Exp Ther* 243: 1035–1042.
- Lemos VS, Côrtes SF, Silva DMR, Campagnole-Santos MJ, Santos RAS (2002). Angiotensin-(1-7) is involved in the endothelium-dependent modulation of phenylephrine-induced contraction in the aorta of mRen-2 transgenic rats. *Br J Pharmacol* 135: 1743–1748.
- Lolait S, Bichet D, Bouvier M, Chini B, Gimpl G, Guillon G, *et al.* (2018) Vasopressin and oxytocin receptors: V_{1A} receptor. IUPHAR/BPS Guide to PHARMACOLOGY. Available at <http://www.guidetopharmacology.org/GRAC/ObjectDisplayForward?objectId=366> (accessed 2018 Feb 25).
- Mauger J-P, Poggioli J, Guesdon F, Claret M (1984). Noradrenaline, vasopressin and angiotensin increase Ca²⁺ influx by opening a common pool of Ca²⁺ channels in isolated rat liver cells. *Biochem J* 221: 121–127.
- McGrath JC, Lilley E (2015). Implementing guidelines on reporting research using animals (ARRIVE etc.): new requirements for publication in BJP. *Br J Pharmacol* 172: 3189–3193.
- McPherson GA, Krstew E, Malta E (1985). Effects of phenoxybenzamine on responses to some receptor agonists and calcium in vitro. *Clin Exp Pharmacol Physiol* 12: 455–464.
- Moric-Janiszewska E, Głogowska-Ligus J, Paul-Samojedny M, W glarz L, Markiewicz-Łoskot G, Szydłowski L (2011). Age- and sex-dependent mRNA expression of KCNQ1 and HERG in patients with long QT syndrome type 1 and 2. *Arch Med Sci* 7: 941–947.
- Mulvany MJ, Halpern W, Mulvany MJ, Halpern W (1977). Contractile properties of small arterial resistance vessels in spontaneously hypertensive and contractile properties of small arterial resistance vessels in spontaneously hypertensive and normotensive rats. *Circ Res* 41: 19–26.
- Nguyen T, Mouksassi M-S, Holford N, Al-Huniti N, Freedman I, Hooker A *et al.* (2017). Model evaluation of continuous data pharmacometric models: metrics and graphics. *CPT Pharmacometrics Syst Pharmacol* 6: 87–109.
- Nyborg NC, Bevan JA (1988). Increased α -adrenergic receptor affinity in resistance vessels from hypertensive rats. *Hypertension* 11: 635–638.
- Oriowo MA, Bevan JA, Bevan RD (1989). Variation in sensitivity of six cat and six rat arteries to norepinephrine can be related to differences in agonist affinity and receptor reserve. *J Pharmacol Exp Ther* 251: 16–20.
- Pérez-Rivera AA, Hlavacova A, Rosario-Colón LA, Fink GD, Galligan JJ (2007). Differential contributions of α -1 and α -2 adrenoceptors to vasoconstriction in mesenteric arteries and veins of normal and hypertensive mice. *Vascul Pharmacol* 46: 373–382.
- Perez D, Bond RA, Bylund DB, Eikenburg DC, Hieble JP, Hills R, *et al.* (2018) Adrenoceptors: α _{1A}-adrenoceptor. IUPHAR/BPS Guide to PHARMACOLOGY. Available at <http://www.guidetopharmacology.org/GRAC/ObjectDisplayForward?objectId=22> (accessed 2018 Feb 25).
- Ponzano S, Blake K, Bonelli M, Enzmann H, on behalf of the European Medicines Agency Committee for Human Medicinal Products First-in-Human Guideline Drafting Group (2018). Promoting safe early clinical research of novel drug candidates: a European Union regulatory perspective. *Clin Pharmacol Ther* 103: 564–566.
- Prins BA, Weber MA, Purdy RE (1992). Norepinephrine amplifies angiotensin II-induced vasoconstriction in rabbit femoral artery. *J Pharmacol Exp Ther* 262: 198–203.
- Ru XC, Qian LB, Gao Q, Li YF, Bruce IC, Xia Q (2008). Alcohol induces relaxation of rat thoracic aorta and mesenteric arterial bed. *Alcohol* 43: 537–543.
- Scaramellini C, Bennett G, Leff P (1997). Analysis of agonist–agonist interactions: the crucial influence of curve shape. *J Pharmacol Toxicol Methods* 37: 167–178.
- Segarra G, Medina P, Vila JM, Chuan P, Domenech C, Lluch S (2002). Increased contraction to noradrenaline by vasopressin in human renal arteries. *J Hypertens* 20: 1373–1379.
- Serradeil-Le Gal C, Herbert JM, Delisee C, Schaeffer P, Raufaste D, Garcia C *et al.* (1995). Effect of SR-49059, a vasopressin V_{1a} antagonist, on human vascular smooth muscle cells. *Am J Physiol Heart Circ Physiol* 268: H404–H410.
- Stam WB, Van der Graaf PH, Saxena PR (1999). Analysis of α 1L-adrenoceptor pharmacology in rat small mesenteric artery. *Br J Pharmacol* 127: 661–670.
- Stam WB, Van der Graaf PH, Saxena PR (1998). Characterization of receptors mediating contraction of the rat isolated small mesenteric artery and aorta to arginine vasopressin and oxytocin. *Br J Pharmacol* 125: 865–873.
- Streefkerk JO, Pfaffendorf M, Van Zwieten PA (2003). Vasopressin-induced facilitation of adrenergic responses in the rat mesenteric artery is V₁-receptor dependent. *Auton Autacoid Pharmacol* 23: 35–41.

Vågnes BØB, Hansen FH, Christiansen REF, Gjerstad C, Iversen BM (2004). Age-dependent regulation of vasopressin V1a receptors in preglomerular vessels from the spontaneously hypertensive rat. *Am J Physiol Renal Physiol* 286: F997–F1003.

Van der Graaf P, Benson N (2018). The role of quantitative systems pharmacology (QSP) in the design of first-in-human trials. *Clin Pharmacol Ther.* <https://doi.org/10.1002/cpt.1145>.

Van der Graaf PH, Shankley NP, Black JW (1996). Analysis of the effects of α 1-adrenoceptor antagonists on noradrenaline-mediated contraction of rat small mesenteric artery. *Br J Pharmacol* 118: 1308–1316.

Van der Graaf PH, Stam WB (1999). Analysis of receptor inactivation experiments with the operational model of agonism yields correlated estimates of agonist affinity and efficacy. *J Pharmacol Toxicol Methods* 41: 117–125.

Van Hasselt JGC, Van Der Graaf PH (2015). Towards integrative systems pharmacology models in oncology drug development. *Drug Discov Today Technol* 15: 1–8.

Yamada S, Suzuki M, Tanaka C, Mori R, Kimura R, Inagaki O *et al.* (1994). Comparative study on α 1-adrenoceptor antagonist binding in human prostate and aorta. *Clin Exp Pharmacol Physiol* 21: 405–411.